Separation Science and Technology
Publication details, including instructions for authors and subscription information:
http://www.informaworld.com/smpp/title~content=t713708471

Solutal Separation under Centrifugation

Li Ning; Roberto Camassa; Robert E. Ecke; Francesco Venneri

To cite this Article Ning, Li , Camassa, Roberto , Ecke, Robert E. and Venneri, Francesco(1998) 'Solutal Separation under Centrifugation', Separation Science and Technology, 33: 4, 551 — 567
To link to this Article: DOI: 10.1080/01496399808544996
URL: http://dx.doi.org/10.1080/01496399808544996

SEPARATION SCIENCE AND TECHNOLOGY, 33(4), pp. 551–567, 1998

Solutal Separation under Centrifugation

LI NING
MATERIAL SCIENCE AND TECHNOLOGY DIVISION MST-10
and
CENTER FOR NONLINEAR STUDIES

ROBERTO CAMASSA
THEORETICAL DIVISION T-7
and
CENTER FOR NONLINEAR STUDIES

ROBERT E. ECKE*
MATERIAL SCIENCE AND TECHNOLOGY DIVISION MST-10
and
CENTER FOR NONLINEAR STUDIES

FRANCESCO VENNERI
ADTT

LOS ALAMOS NATIONAL LABORATORY
LOS ALAMOS, NEW MEXICO 87545, USA

ABSTRACT

We report on experiments and numerical simulations of the centrifugal separation of solutes in aqueous solutions. The experiments are measurements of solutal concentrations in binary and ternary aqueous mixtures of seven different salts subject to centrifugal accelerations of between 57,000g and 200,000g. The evolution of the concentration profiles are measured and the sedimentation coefficients are determined. We compare our experimentally determined coefficients with those predicted by the Svedberg relation. Our numerical simulations of the diffusion and sedimentation dynamics of centrifugation agree well with the experiments and constitute a basis for a nonequilibrium centrifugal separation scheme.

* To whom correspondence should be addressed.

1. INTRODUCTION

The physical separation of liquid solutions by strong centrifugal accelerations is a technique that has not been investigated actively because chemical techniques are often available and are usually much more efficient. Thus, although the theoretical foundations for such separations were established over three decades ago (1, 2), there is little direct experimental work reported in the literature that verifies the solutal separation in simple miscible solutions (3, 4). In particular, few results are available that address the dynamic behavior of how a solutal concentration gradient is established. A vast literature exists, however, on centrifugal separation in biological systems for which ultrahigh-speed centrifuges ("ultracentrifuges") are commonly used for separating solutions containing very large molecules (5). Single solutal gradients are also routinely used in centrifugal separations (5). Recently, the potential advantages of physical separation of solutions of nuclear material has renewed interest in centrifugal separation effects (6, 7). Unlike chemical techniques, physical separation methods do not offer the means of isolating high-purity nuclear material and are thus favorable for nonproliferation reasons.

In this paper we report theoretical, numerical, and experimental results on mass transport resulting from centrifugal acceleration of binary and ternary mixtures. In particular, we concentrate on the dynamic evolution of solute concentration, an issue that is clearly of paramount importance for practical applications. An interesting implication of our results is that technologically useful separations can be achieved long before reaching an equilibrium concentration profile.

We first describe the theoretical foundations for centrifugal separation in Section 2. In Section 3 we present experimental measurements of the separation of constituents of binary and ternary mixtures of a variety of salts dissolved in water, and compare them with numerical simulations. These comparisons yield values of the sedimentation and diffusion coefficients for $HAuCl_4$, $CuSO_4$, CsCl, $ErCl_3$, $SrCl_2$, $LaCl_3$, and NaCl. These experimental values are compared with predictions of the Svedberg relation which relates the sedimentation coefficient and the mass diffusivity.

2. THEORETICAL MODEL

The bases for a theory of molecular separation by centrifugal forces are the equations of mass and heat transport (8). For the present purposes it is sufficient to consider isothermal situations and assume that heat transport is unimportant. In this case the basic equation for isothermal centrifugation in a sector-shaped centrifuge or a cylindrical annulus is the so-

called Lamm differential equation (2):

$$\frac{\partial c}{\partial t} = \frac{1}{r}\frac{\partial}{\partial r}\left(rD\frac{\partial c}{\partial r} - s\Omega^2 r^2 c\right) \tag{1}$$

Here we assume that the mass diffusion coefficient D and the sedimentation coefficient s are independent of the radial position r (see Fig. 1) or, equivalently, that the coefficients are independent of pressure and concentration. This condition is typically well satisfied for dilute solutions. The boundary conditions are such that there is no mass flux across the end surfaces:

$$\frac{1}{c}\frac{\partial c}{\partial r}\bigg|_{r_i} = \frac{s\Omega^2}{D} r_i, \qquad i = 1, 2 \tag{2}$$

where r_1 and r_2 correspond respectively to the inner and outer radii of the cylinder. The steady-state solution to Eq. (1), which can be readily computed by taking $\partial c/\partial t = 0$ in Eq. (1) and integrating the resulting ordinary differential equation, is known as the Archibald solution (2) and describes the equilibrium concentration profile:

$$\frac{c(\varrho)}{c_0} = \frac{(\varrho_2 - \varrho_1)}{[\exp(\varrho_2) - \exp(\varrho_1)]}\exp(\varrho) \tag{3}$$

where $\varrho = s\Omega^2 r^2/2D$, $\varrho_i = s\Omega^2 r_i^2/2D$ for $(i = 1, 2)$. This equilibrium profile

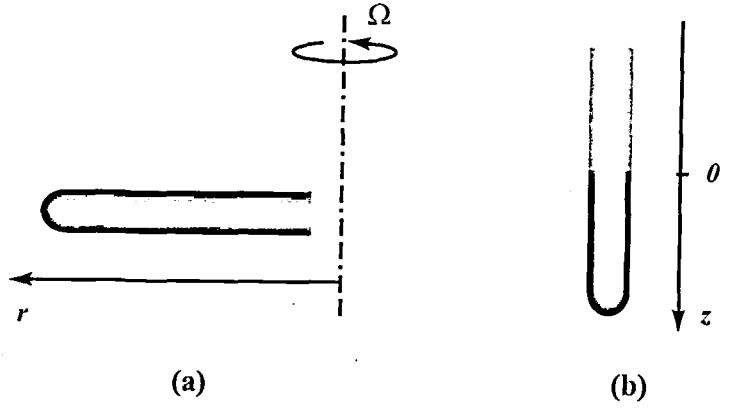

FIG. 1 (a) Cylindrical coordinate for vials during centrifugation. (b) Solution depth coordinate in the diffusion experiment.

can be used to estimate the ratio of concentrations that can be achieved for a given solution and rotation rate, but information about the time scale for achieving equilibrium requires consideration of the dynamic equations.

It is useful to rewrite the Lamm differential equation in dimensionless form. We nondimensionalize Eq. (1) by using a characteristic mass diffusion time $\tau \equiv t/(d^2/D)$ and a characteristic length $\xi \equiv r/d$ where d is the annular gap distance $r_2 - r_1$,

$$\frac{\partial \theta}{\partial \tau} = \frac{1}{\xi}\frac{\partial}{\partial \xi}\left(\xi \frac{\partial \theta}{\partial \xi} - S\xi^2\theta\right) \tag{4}$$

where $\theta \equiv c/c_0$ and $S \equiv (s/D)\Omega^2 d^2$ are dimensionless numbers. This description can be used to classify the numerical-simulation results using one combined parameter S for a given geometry. A very useful result from this classification can be stated as follows: a higher S results in a steeper concentration gradient, and a larger D with a fixed S leads to a higher sedimentation speed. This criterion can be used profitably in understanding qualitatively the sedimentation process.

The theoretical analysis for nonsector-shaped centrifuges is more difficult owing to the interaction between radial sedimentation and sidewalls (2). For example, hydrodynamic flows are possible in these situations. Assuming that their effects are small (4), we ignore these possibilities and derive the sedimentation equation for a vial with constant cross-sectional area aligned along the radial direction (the configuration in our experiments):

$$\frac{\partial c}{\partial t} = \frac{\partial}{\partial r}\left(D\frac{\partial c}{\partial r} - s\Omega^2 rc\right) \tag{5}$$

The boundary conditions are the same as in Eq. (2). The equilibrium solution is similar to the Archibald solution:

$$\frac{c(r)}{c_0} = \frac{r_2 - r_1}{\int_{r1}^{r_2} \exp(s\Omega^2 z^2/2D)\, dz} \exp\left(\frac{s\Omega^2}{2D} r^2\right) \tag{6}$$

Equation (5) can be nondimensionalized in the same way as for Eq. (4) to obtain

$$\frac{\partial \theta}{\partial \tau} = \frac{\partial}{\partial \xi}\left(\frac{\partial \theta}{\partial \xi} - S\xi\theta\right) \tag{7}$$

The time scale in Eqs. (4) and (7) is inversely proportional to D, which can be determined from an independent experiment. Some of these data

are available from the literature but we repeated several measurements of D as an independent check on our fluid-extraction measurement method. A simple argument based on the solution of the one-dimensional diffusion equation relates D to concentration gradients. For an infinite system and an initial concentration profile of $c = 0$ for $z < 0$ and $c = c_0$ for $z > 0$, the solution is an error function erf(z) of the form:

$$\frac{c(z)}{c_0} = \frac{1}{2\sqrt{\pi Dt}} \int_{-\infty}^{z} dz' \exp\left(-\frac{z'^2}{4Dt}\right) \tag{8}$$

It is more convenient for analyzing the experimental data to consider the derivative of erf(z) which is a Gaussian:

$$\frac{1}{c_0}\frac{dc(z)}{dz} = \frac{1}{2\sqrt{\pi Dt}} \exp\left(-\frac{z^2}{4Dt}\right) \tag{9}$$

We will use this form in Section 3 to extract D from experimental data.

We take Eqs. (1) and (3) as the starting point for a numerical study of the equilibrium concentration profiles and the dynamics of the separation process. Before comparing the numerical results with our experiments, we should address the validity of our assumptions in light of the potentially large pressure gradients generated by centrifugal accelerations as high as 200,000g. The most likely problem, especially for the highest rotation rates, is that the coefficients in Eq. (1) depend on r through the pressure and concentration. Other possible problems are small deviations in the geometry (for example, the vials in the experiments had spherical bottoms rather than flat ones) and nondilute concentrations. The qualitative features of the sedimentation dynamics do not, however, depend heavily on these minor corrections. As we will see below, the present formulation of the theory describes our experimental results very well.

The numerical simulations used a partial-differential-equation-solver package (9). The equations were integrated in time with a variable-order, variable-timestep ordinary differential equation solver to a tolerance of 10^{-8} per unit time. The spatial operators were approximated with second-order finite-difference methods on a uniform grid. The number of spatial points was varied between 50 and 400 to ensure that the numerical results were converged; typically we used 100 points. For purpose of comparison with the experiments, Eq. (7) was simulated. Extensive simulations of Eq. (4) were also performed to model possible applications (10, 11). The dynamics dictated by the two equations do not differ greatly.

Without explicit measurement of the equilibrium profile under centrifugation, the sedimentation coefficient is often estimated from known values

of D using the Svedberg equation which is valid in the infinitely dilute limit,

$$\frac{s}{D} \equiv \frac{\rho k_p}{(pc)} = \frac{M_s(1 - \rho_0/\rho_s)}{nRT} \tag{10}$$

where M_s and ρ_s are respectively the molecular weight and density of the solute, ρ_0 is the density of the solvent, n is the so-called dissociation number for electrolyte solutions (1 for nonelectrolyte solutions), R is the gas constant, and T is the absolute temperature. This relation also assumes that the partial volumes of the components in the solutions do not change upon mixing. The most important corrections to this simple relation stem from the concentration-corrected mass diffusivities for nondilute solutions. For nonelectrolyte solutions, nonideality correction is modeled by a multiplicative factor, $1/(1 + c(\partial \ln y_s/\partial c)_{T,p})$, on the right-hand side, where y_s is the activity coefficient of the solute. For electrolyte solutions the dissociation of ions is a further complication. To model this effect, a factor called the dissociation number is usually introduced. It corresponds to the number of ions dissociated from one solute molecule in the solution and multiplies the denominator on the right-hand side of Eq. (10). Because we extract the ratio s/D and D directly from experiment, we need not use Eq. (10). We will, however, make comparisons between our results and those obtained assuming the Svedberg relation.

3. EXPERIMENTS AND COMPARISONS WITH NUMERICAL SIMULATIONS

In the experiments we measured the concentration profiles established by centrifugal acceleration and determined the dynamics of sedimentation. We used a commercial preparative ultracentrifuge (12) capable of rotation speeds up to 41,000 revolutions per minute. Aqueous solutions of $HAuCl_4$, $CuSO_4$, CsCl, $ErCl_3$, $SrCl_2$, $LaCl_3$, and NaCl were prepared with molar concentrations of less than 5%. We also prepared dilute ternary solutions of CsCl and NaCl in water. Most of our results are for CsCl which has long been a favorite of the biomedical community for establishing known density gradients for separation of large molecules (5). The centrifuge had a swing-bucket rotor with six metallic vessels. Soft chemically-inert plastic vials containing the solutions were placed into the vessels, and the vessels were sealed against the centrifuge vacuum which was typically less than 10 μm. Once good vacuum was achieved in the centrifuge, the rotor was spun up to the operating rotation rate in about 5–10 minutes. During operation the rotor was temperature controlled at about 25°C. After some time at full speed the rotor was decelerated, the system was repressurized, and the samples were removed for measurement. Several

precautions were taken to ensure undisturbed separation. Inadequate vacuum or too rapid deceleration could result in mixing which could destroy the centrifugally induced concentration gradient. The latter was the most troublesome, completely destroying the separation effect if the system brake was used to decelerate the centrifuge below 10,000 rpm. Instead we turned off the brake and let the rotor decelerate under the influence of the natural friction that arises from a variety of sources including bearing friction and viscous drag. This increased the spin-down time from about 5 minutes to about 30 minutes. Even with this precaution some mixing might have occurred during spin-down although our measurements suggest this was a small effect when we used the above procedure. Finally, one might be concerned that the separated solution could backdiffuse during the deceleration and measurement phase. This effect was studied earlier (3) and was shown to degrade the profiles primarily near the boundaries. Evidence for this is seen in our experimental concentration profiles as well as in our numerical simulations. [Indeed, a simple argument based on the Lamm equation (Eq. 1) and its boundary conditions (Eq. 2) or the analogous equation (Eq. 5) shows that the time derivative of the concentration is largest at the boundary owing to a time-varying centrifugal field.] With this limitation in mind, one should consider our measurements to be a lower bound on the sedimentation efficiency. This is the primary uncertainty in our measurements as reflected in the error assigned to our determination of s. Other sources of uncertainty in our measurements are the sedimentation that occurs during spin-up and spin-down of the centrifuge and hydrodynamic/thermal mixing effects. The former influence should be less than 5% since the separation times were much longer than the transients before and after the constant Ω interval.

Once the solution was sedimented under the action of the centrifugal force, the concentration profile was measured using the density dependence of the index of refraction. The vial containing the solution was removed from the metal container and a small amount of solution was extracted from different heights using a syringe. The depth from which the fluid was taken corresponded to a radial position when the vial was being rotated. A superior method, using a peristaltic pump and a fraction collector, was also used for some of the measurements and improved the reproducibility of our measurements. Both methods, however, gave quite good results as we now show. A recent study comparing the technique of fluid extraction after discrete time intervals in a preparative centrifuge with an in-situ continuous measurement of density using optical methods in an analytical centrifuge showed that the two methods yield comparable results except for some degradation of the endwall profile owing to backdiffusion (4).

The concentration of each sample was determined using a commercial refractometer (13) capable of resolving differences in index of refraction of about ± 0.0001 out of 1.4000. The sample volume was temperature controlled at 25°C using a refrigerator/circulator. The concentration was calibrated against density according to published data (3) or our own calibration results. Normalizing by the initial radially-uniform concentration c_0, we obtain the quantity $c(r,t)/c_0$. The measurements for different total times allow a determination of the dynamics at a modest number of discrete times.

We also independently determined D by preparing a layer of aqueous solution with concentration c_0 stratified below a layer of pure water in a vertical vial. This initial condition evolved under the action of mass diffusion so that in several hours the concentration profile had a sigma-function shape. Such a profile is shown in Fig. 2 for CsCl along with the center-difference derivatives of the experimental data and a fit to a Gaussian function of the form of Eq. (9) from which one obtains $D = 1.7 \pm 0.2 \times 10^{-5}$ cm^2/s. The value of D for CsCl compares reasonably with the published data ($D \approx 1.95 \times 10^{-5}$ cm^2/s) (14). For NaCl a similar experiment found $D = 1.7 \pm 0.2 \times 10^{-5}$ cm^2/s, which also agrees reasonably with the published result ($D \approx 1.5 \times 10^{-5}$ cm^2/s) (15). This exercise also verifies our experimental procedure of fluid extraction for measuring sedimentation profiles.

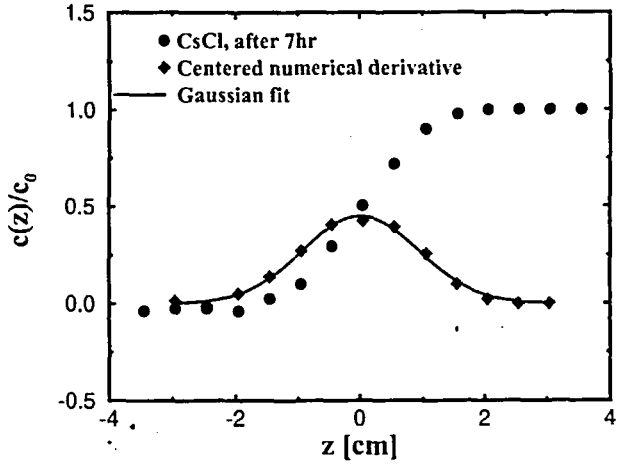

FIG. 2 $c(z)/c_0$ (●) vs z for CsCl, numerical derivative (◆), and fit to Gaussian function (——).

The results of one centrifugation run at 25,000 rpm and lasting 135.6 hours for several different solutions are in Fig. 3, which shows the concentration profiles for $HAuCl_4$ (the initially uniform molar fraction x_0 = 0.0022, M = 340), CsCl (x_0 = 0.032, M = 168.4), and NaCl (x_0 = 0.029, M = 58.4). The difference in the profiles reflects the difference in the material properties: $HAuCl_4$, with the heaviest molecular weight and thus the highest sedimentation coefficient, had the steepest concentration gradient; NaCl, being the lightest, established a very gentle profile while the resultant gradient for CsCl was in the middle. The profiles, measured for times long enough that they are close to equilibrium, of four additional salt solutions, $CuSO_4$ (x_0 = 0.014, M = 159.6), $ErCl_3$ (x_0 = 0.0094, M = 273.7), $LaCl_3$ (x_0 = 0.0065, M = 245.3), and $SrCl_2$ (x_0 = 0.0094, M = 158.5), are shown in Fig. 4. These solutions were separated at a higher rotation rate, Ω = 35,000 rpm for 204 hours. From these profiles we obtain the ratios s/D from fits to Eq. (6). The results are tabulated in Table 1. We estimate that the errors in D and s/D are roughly 20%.

We can compare the measured values of s/D to those predicted from the Svedberg relation using known values of n, the dissociation number, which in general equals the number of ions one electrolyte solute molecule dissociates into a solution. The agreement between the measured s/D and those obtained using the Svedberg relation are within experimental uncertainty for most of the salt solutions. The exceptions are for higher

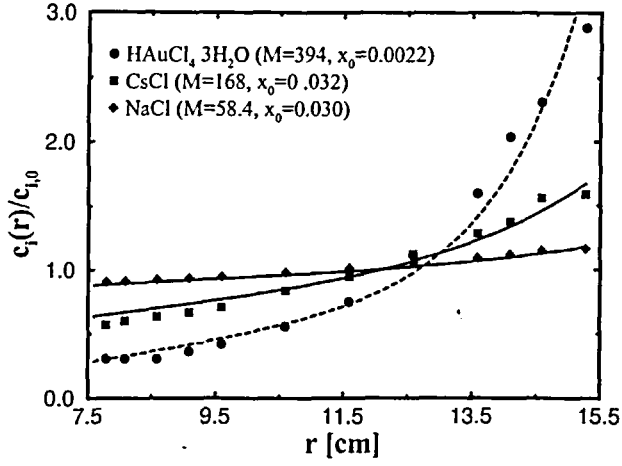

FIG. 3 Equilibrium profiles $c(r)/c_0$ vs r for $HAuCl_4$, CsCl, and NaCl with Ω = 25,000 rpm. The solid lines are from simulations, and the dashed line is a guide to the eye.

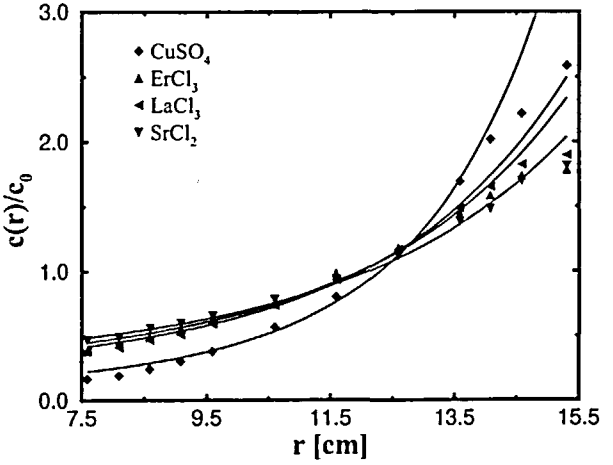

FIG. 4 Near equilibrium profiles $c(r)/c_0$ vs r for $CuSO_4$, $ErCl_3$, $LaCl_3$, and $SrCl_2$. The solid lines are fits to equilibrium solutions excluding end effects.

initial concentrations of CsCl (c_0 = 0.232) and $ErCl_3$ (c_0 = 0.177) which show lower than expected values of s/D. This decrease for higher concentration solutions is consistent with the sign of first-order corrections to Eq. (10), but without additional measurements as a function of concentration it is hard to be sure of the nature of the discrepancy.

TABLE 1
Type of Salt Solution, c_0, D (from experiment), (s/D) (from experiment), (s/D) (from Svedberg relation), and n for Ω = 35,000 rpm

Salt	c_0	D (10^{-5} cm^2/s)	$(s/D)_{exp}$ (10^{-9} s^2/cm^2)	$(s/D)_{Svedberg}$ (10^{-9} s^2/cm^2)	n
$HAuCl_4$[a]	0.0403	1.5 ± 0.3	5.3 ± 1.2	5.1	2
$CuSO_4$	0.111	0.41 ± 0.08	2.4 ± 0.5	2.3	2
CsCl[a]	0.232	1.7 ± 0.3	1.9 ± 0.4	2.5	2
CsCl	0.086	1.9 ± 0.4	2.5 ± 0.5	2.5	2
$ErCl_3$	0.177	0.90 ± 0.2	1.4 ± 0.3	2.1	4
$LaCl_3$	0.081	0.78 ± 0.2	1.5 ± 0.3	1.8	4
$SrCl_2$	0.077	0.99 ± 0.2	1.2 ± 0.2	1.4	3
NaCl[a]	0.089	1.7 ± 0.3	[b]	0.63	2

[a] Ω = 25,000 rpm.
[b] Not fully equilibrated.

The experiments on the separation dynamics show good qualitative agreement with expectations derived from the numerical simulations. We have collected data on the dynamics for aqueous solutions of NaCl (x_0 = 0.03, M = 58.4), CsCl (x_0 = 0.032, M = 168.4), and $HAuCl_4$ (x_0 = 0.0022, M = 340; the crystal form before dissolution is $HAuCl_4 \cdot 3H_2O$). As shown in Figs. 5, 6, and 7, there is a plateau region at short times that softens with increasing time. The qualitative features of these data are the same as for the simulations.

The comparison can be made more quantitative with the numerical simulations using the available or measured material parameters. In choosing the parameters for simulating sedimentation dynamics, we used published data whenever possible. The only exception is the sedimentation coefficient for the CsCl centrifugation experiment at 25,000 rpm. Since we obtained a series of concentration profiles, we adopted a method verified with numerical simulations to determine the equilibrium concentration profile from the time series by fitting $c(r_i,t)$ at each r_i, to an exponential plus an offset. This profile is then fitted with the solution of Eq. (6) for a cylindrical vial. The ratio of the sedimentation coefficient to the diffusion coefficient was then used in the simulation. This procedure produced a somewhat smaller value for the sedimentation coefficient than the published result (4). Nevertheless, the simulated sedimentation dy-

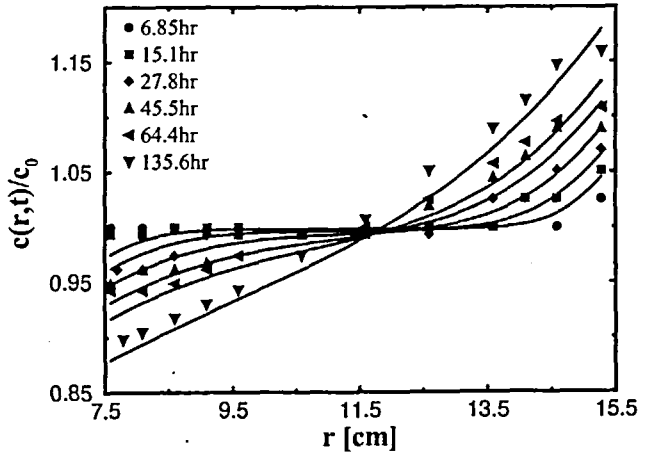

FIG. 5 $c(r,t)/c_0$ vs r for NaCl with total separation times of 6.8 h, 15.1 h, 27.8 h, 45.2 h, 64.4 h, and 135.6 h. The solid lines are simulated with $s = 9.5 \times 10^{-15}$ s, $D = 1.5 \times 10^{-5}$ cm^2/s.

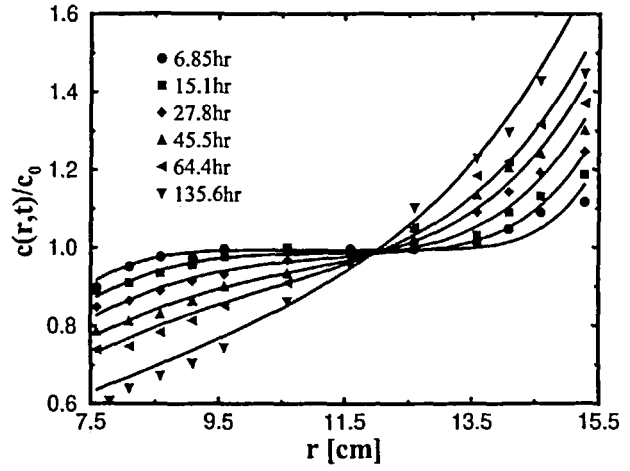

FIG. 6 $c(r,t)/c_0$ vs r for CsCl with total separation times of 6.8 h, 15.1 h, 27.8 h, 45.2 h, 64.4 h, and 135.6 h. The solid lines are simulated with $s = 3.7 \times 10^{-14}$ s, $D = 1.95 \times 10^{-5}$ cm^2/s.

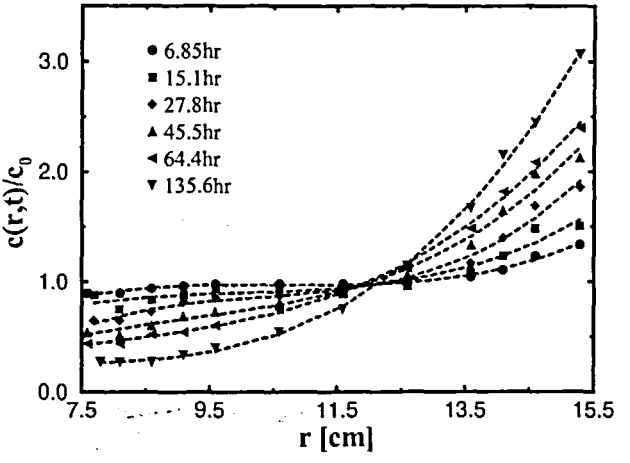

FIG. 7 $c(r,t)/c_0$ vs r for $HAuCl_4$ with total separation times of 6.8 h, 15.1 h, 27.8 h, 45.2 h, 64.4 h, and 135.6 h. The dashed lines are guides to the eye.

namics compares favorably with the experiment, perhaps owing to the inclusion of some systematic experimental procedural artifacts such as mixing during decelerating and before measurement. The results of the simulations are shown in Fig. 5 for NaCl and in Fig. 6 for CsCl. The general agreement is very reasonable.

We also conducted the centrifugal experiments on a ternary aqueous solution of CsCl and NaCl. We prepared the solution and its control samples in the following way: solutions of CsCl and NaCl were separately made with molar concentrations of 3.2 and 3.0%. We then mixed two equal volumes of the two solutions to get the ternary mixture. The CsCl (NaCl) control solution was made by mixing equal volumes of the binary CsCl (NaCl) solution with water. The control samples then had approximately the same concentrations of the solutes as in the ternary mixture. The three samples were loaded into the centrifuge and run at 35,000 rpm for 46 hours. After the centrifugation, the sample solutions were partitioned using a peristaltic pump and a fraction collector into 20 vials. The collected solutions were then used to measure the refractive indices and specific densities. Figure 8 shows the measured refractive indices versus radial distances for the ternary mixture and the control samples. The important result is that the sum of the refractive indices of the control samples minus the refractive index of water (its contribution is doubly counted

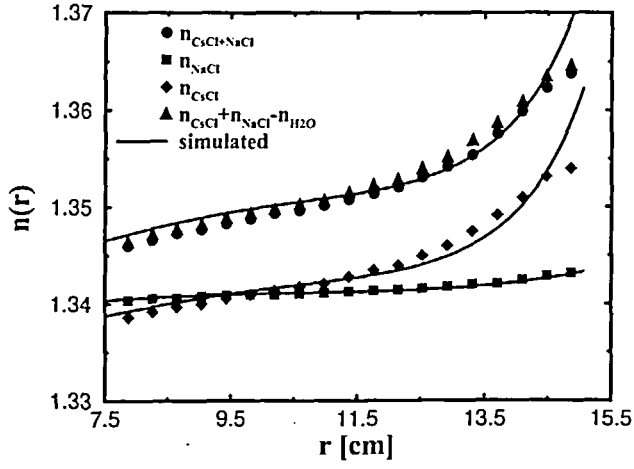

FIG. 8 The measured refractive indices for the ternary mixture of CsCl and NaCl in water and the control samples. The solid lines are from simulations with published material properties.

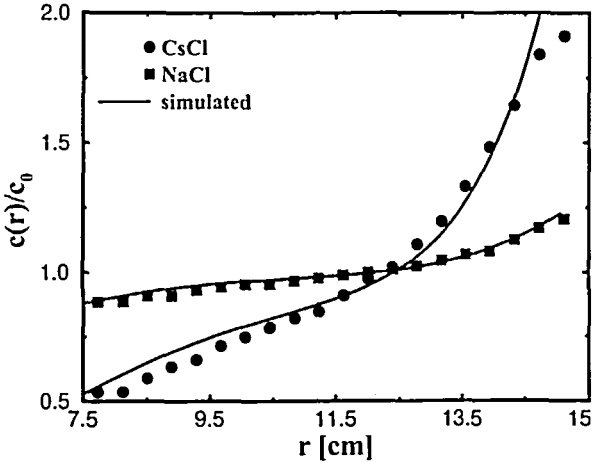

FIG. 9 The concentrations of CsCl and NaCl versus radial distances inferred from the control samples. The solid lines are from simulations using the published material properties: $s = 5.1 \times 10^{-14}$ s, $D = 1.88 \times 10^{-5}$ cm^2/s for CsCl; $s = 9.5 \times 10^{-15}$ s, $D = 1.5 \times 10^{-5}$ cm^2/s for NaCl.

in the sum) coincides with the refractive index of the ternary mixture at each corresponding radial distance, validating the theoretical prediction that, under centrifugation, a dilute multicomponent solution behaves like the sum of individual binary solutions (16). Figure 9 shows the normalized concentrations of CsCl and NaCl in the ternary mixture inferred from the control samples. The separation is clearly quite significant. This experimental result compares favorably with the simulations using the published material properties, as shown in the respective figures.

CONCLUSIONS

We have presented experimental and numerical results on the dynamics and equilibrium profiles of centrifugal separation where diffusion is important (mass diffusion can usually be neglected for the sedimentation of large molecules of biological interest). In particular, we have measured the process of centrifugation of both binary and ternary aqueous salt solutions of varying molecular weight. We have determined the ratio of the sedimentation coefficient s and the mass diffusion coefficient D for seven different aqueous solutions of chloride salts. Most of the solutions have values of s/D consistent with the predictions of the Svedberg relation with

the possible exception of those with higher initial concentrations (CsCl, $c_0 = 0.232$; $ErCl_3$, $c_0 = 0.177$). The general agreement between experiments and simulation is very good. We have demonstrated that significant separation of solutes in solutions can be achieved in times much shorter than the time to reach equilibrium. We have also validated the theoretical prediction on dilute multicomponent solutions that they behave essentially as the sum of the independent binary solutions.

The technological application of these concepts to physical separation of materials in a solution should be important to the nuclear energy industry, where chemical reprocessing of nuclear fuel and the disposal of nuclear waste are major concerns. In this context there are other issues that need to be addressed. Since high rates of separation are desirable, the operating conditions will be at the largest rotation rates that can be achieved technologically. At these limits the effects of pressure on the parameters in the models might be important and need to be evaluated. Next, it might be advantageous to work at larger concentrations in some applications so that an investigation of separation for nondilute solutions would be required. Finally, a wider range of materials from strong and weak electrolytes to liquid metals should be studied in order to assess whether our analysis and measurements are representative of the general behavior of solution separation under centrifugal forces. Clearly, much work needs to be done in these directions. In particular, while the theoretical literature is relatively well established, very few experimental results are available to validate the theory. The study presented here can be considered as a starting point along this program, but it has already demonstrated that the fundamentals of centrifugation for dilute solutions are established well enough for many applications.

NOMENCLATURE

c	weight-percent concentration
c_0	initial value of c
d	annular gap
D	mass diffusivity
g	acceleration of gravity
k_p	baro-diffusion coefficient
n	dissociation number
M	molecular weight
M_s	molecular weight of solute
p	pressure
r	radius measured from rotation axis
r_1	inner radius of annulus

r_2	outer radius of annulus
R	gas constant
s	sedimentation coefficient
S	dimensionless sedimentation $(s/D)\ \Omega^2 d^2$
t	time
T	temperature
x	molar concentration
x_0	initial molar concentration
y_s	activity coefficient
z, z'	solution depth
ξ	dimensionless length
Ω	rotation rate
θ	c/c_0
ρ	density
ρ_0	density of pure solvent
ρ_s	density of solute
τ	dimensionless mass diffusion time
ϱ	Archibald parameter $s\Omega^2 r^2/2D$

ACKNOWLEDGMENTS

We acknowledge Charles Bowman for his motivating ideas about technological applications of centrifugal separation. We also thank J. M. Hyman and D. Stark for assistance with the numerical simulations and Richard Reynolds for helping us make several initial measurements of separation. This project was funded by the U.S. DOE.

REFERENCES

1. T. Svedberg and K. O. Pedersen, *The Ultracentrifuge*, Clarendon Press, Oxford, 1940.
2. H. Fujita, *Mathematical Theory of Sedimentation Analysis*, Academic Press, New York, NY, 1962.
3. J. Ifft, D. Voet, and J. Vinograd, *J. Phys. Chem.*, *65*, 1138 (1961).
4. A. Minton, *Biophys. Chem.*, *42*, 13 (1992).
5. H.-W. Hsu, in *Separations by Centrifugal Phenomena* (Vol. 16 of Techniques of Chemistry, edited by E. S. Perry), Wiley, New York, NY, 1981.
6. C. Bowman, *Technical Report*, *LA-UR-92-1065*, Los Alamos National Laboratory.
7. F. Venneri, *Technical Report*, *LA-UR-95-213*, Los Alamos National Laboratory.
8. L. D. Landau and E. M. Lifshitz, *Fluid Mechanics*, Pergamon, Oxford, 1959.
9. An early version of the software package PDELIB is described in *Los Alamos Technical Report LA-UR-79-740* by J. M. Hyman.
10. L. Ning, R. Camassa, R. Ecke, and F. Venneri, in *Proceedings of 1st International Conference on Accelerator Driven Transmutation Technologies and Applications, Las Vegas, NV*, AIP Press, Woodbury, NY, 1995.

11. L. Ning, R. Camassa, R. Ecke, and F. Venneri, in *Proceedings of International Conference on Evaluation of Emerging Nuclear Fuel Cycle Systems*, Images et formes, Versailles, France, 1995.
12. Model L3-50 Ultracentrifuge with SW-41 Ti Rotor, Beckmann.
13. Model ABBE-3C refractometer, Milton Roy.
14. R. A. Robinson and R. H. Stokes, *Electrolyte Solutions*, Academic Press, New York, NY, 1959.
15. *Handbook of Chemistry and Physics*, CRC Press, Boca Raton, FL, 1983.
16. H. Tyrrell, *Diffusion and Heat Flow in Liquids*, Butterworths, London, 1961.

Received by editor July 25, 1996
Revision received July 1997